Search for the charged lepton flavor violating decay $J/\psi \to e\tau$

M. Ablikim,[1] M. N. Achasov,[10,c] P. Adlarson,[67] S. Ahmed,[15] M. Albrecht,[4] R. Aliberti,[28] A. Amoroso,[66a,66c] M. R. An,[32] Q. An,[63,49] X. H. Bai,[57] Y. Bai,[48] O. Bakina,[29] R. Baldini Ferroli,[23a] I. Balossino,[24a] Y. Ban,[38,k] K. Begzsuren,[26] N. Berger,[28] M. Bertani,[23a] D. Bettoni,[24a] F. Bianchi,[66a,66c] J. Bloms,[60] A. Bortone,[66a,66c] I. Boyko,[29] R. A. Briere,[5] H. Cai,[68] X. Cai,[1,49] A. Calcaterra,[23a] G. F. Cao,[1,54] N. Cao,[1,54] S. A. Cetin,[53a] J. F. Chang,[1,49] W. L. Chang,[1,54] G. Chelkov,[29,b] D. Y. Chen,[6] G. Chen,[1] H. S. Chen,[1,54] M. L. Chen,[1,49] S. J. Chen,[35] X. R. Chen,[25] Y. B. Chen,[1,49] Z. J. Chen,[20,l] W. S. Cheng,[66c] G. Cibinetto,[24a] F. Cossio,[66c] X. F. Cui,[36] H. L. Dai,[1,49] X. C. Dai,[1,54] A. Dbeyssi,[15] R. E. de Boer,[4] D. Dedovich,[29] Z. Y. Deng,[1] A. Denig,[28] I. Denysenko,[29] M. Destefanis,[66a,66c] F. De Mori,[66a,66c] Y. Ding,[33] C. Dong,[36] J. Dong,[1,49] L. Y. Dong,[1,54] M. Y. Dong,[1,49,54] X. Dong,[68] S. X. Du,[71] Y. L. Fan,[68] J. Fang,[1,49] S. S. Fang,[1,54] Y. Fang,[1] R. Farinelli,[24a] L. Fava,[66b,66c] F. Feldbauer,[4] G. Felici,[23a] C. Q. Feng,[63,49] J. H. Feng,[50] M. Fritsch,[4] C. D. Fu,[1] Y. Gao,[38,k] Y. Gao,[64] Y. Gao,[63,49] Y. G. Gao,[6] I. Garzia,[24a,24b] P. T. Ge,[68] C. Geng,[50] E. M. Gersabeck,[58] A. Gilman,[61] K. Goetzen,[11] L. Gong,[33] W. X. Gong,[1,49] W. Gradl,[28] M. Greco,[66a,66c] L. M. Gu,[35] M. H. Gu,[1,49] S. Gu,[2] Y. T. Gu,[13] C. Y. Guan,[1,54] A. Q. Guo,[22] L. B. Guo,[34] R. P. Guo,[40] Y. P. Guo,[9,h] A. Guskov,[29] T. T. Han,[41] W. Y. Han,[32] X. Q. Hao,[16] F. A. Harris,[56] N. Hüsken,[60] K. L. He,[1,54] F. H. Heinsius,[4] C. H. Heinz,[28] T. Held,[4] Y. K. Heng,[1,49,54] C. Herold,[51] M. Himmelreich,[11,f] T. Holtmann,[4] Y. R. Hou,[54] Z. L. Hou,[1] H. M. Hu,[1,54] J. F. Hu,[47,m] T. Hu,[1,49,54] Y. Hu,[1] G. S. Huang,[63,49] L. Q. Huang,[64] X. T. Huang,[41] Y. P. Huang,[1] Z. Huang,[38,k] T. Hussain,[65] W. Ikegami Andersson,[67] W. Imoehl,[22] M. Irshad,[63,49] S. Jaeger,[4] S. Janchiv,[26,j] Q. Ji,[1] Q. P. Ji,[16] X. B. Ji,[1,54] X. L. Ji,[1,49] Y. Y. Ji,[41] H. B. Jiang,[41] X. S. Jiang,[1,49,54] J. B. Jiao,[41] Z. Jiao,[18] S. Jin,[35] Y. Jin,[57] T. Johansson,[67] N. Kalantar-Nayestanaki,[55] X. S. Kang,[33] R. Kappert,[55] M. Kavatsyuk,[55] B. C. Ke,[43,1] I. K. Keshk,[4] A. Khoukaz,[60] P. Kiese,[28] R. Kiuchi,[1] R. Kliemt,[11] L. Koch,[30] O. B. Kolcu,[53a,e] B. Kopf,[4] M. Kuemmel,[4] M. Kuessner,[4] A. Kupsc,[67] M. G. Kurth,[1,54] W. Kühn,[30] J. J. Lane,[58] J. S. Lange,[30] P. Larin,[15] A. Lavania,[21] L. Lavezzi,[66a,66c] Z. H. Lei,[63,49] H. Leithoff,[28] M. Lellmann,[28] T. Lenz,[28] C. Li,[39] C. H. Li,[32] Cheng Li,[63,49] D. M. Li,[71] F. Li,[1,49] G. Li,[1] H. Li,[63,49] H. Li,[43] H. B. Li,[1,54] H. J. Li,[9,h] J. L. Li,[41] J. Q. Li,[4] J. S. Li,[50] Ke Li,[1] L. K. Li,[1] Lei Li,[3] P. R. Li,[31] S. Y. Li,[52] W. D. Li,[1,54] W. G. Li,[1] X. H. Li,[63,49] X. L. Li,[41] Xiaoyu Li,[1,54] Z. Y. Li,[50] H. Liang,[63,49] H. Liang,[1,54] H. Liang,[27] Y. F. Liang,[45] Y. T. Liang,[25] G. R. Liao,[12] L. Z. Liao,[1,54] J. Libby,[21] C. X. Lin,[50] B. J. Liu,[1] C. X. Liu,[1] D. Liu,[63,49] F. H. Liu,[44] Fang Liu,[1] Feng Liu,[6] H. B. Liu,[13] H. M. Liu,[1,54] Huanhuan Liu,[1] Huihui Liu,[17] J. B. Liu,[63,49] J. L. Liu,[64] J. Y. Liu,[1,54] K. Liu,[1] K. Y. Liu,[33] Ke Liu,[6] L. Liu,[63,49] M. H. Liu,[9,h] P. L. Liu,[1] Q. Liu,[54] Q. Liu,[68] S. B. Liu,[63,49] Shuai Liu,[46] T. Liu,[1,54] W. M. Liu,[63,49] X. Liu,[31] Y. Liu,[31] Y. B. Liu,[36] Z. A. Liu,[1,49,54] Z. Q. Liu,[41] X. C. Lou,[1,49,54] F. X. Lu,[16] F. X. Lu,[50] H. J. Lu,[18] J. D. Lu,[1,54] J. G. Lu,[1,49] X. L. Lu,[1] Y. Lu,[1] Y. P. Lu,[1,49] C. L. Luo,[34] M. X. Luo,[70] P. W. Luo,[50] T. Luo,[9,h] X. L. Luo,[1,49] S. Lusso,[66c] X. R. Lyu,[54] F. C. Ma,[33] H. L. Ma,[1] L. L. Ma,[41] M. M. Ma,[1,54] Q. M. Ma,[1] R. Q. Ma,[1,54] R. T. Ma,[54] X. X. Ma,[1,54] X. Y. Ma,[1,49] F. E. Maas,[15] M. Maggiora,[66a,66c] S. Maldaner,[4] S. Malde,[61] Q. A. Malik,[65] A. Mangoni,[23b] Y. J. Mao,[38,k] Z. P. Mao,[1] S. Marcello,[66a,66c] Z. X. Meng,[57] J. G. Messchendorp,[55] G. Mezzadri,[24a] T. J. Min,[35] R. E. Mitchell,[22] X. H. Mo,[1,49,54] Y. J. Mo,[6] N. Yu. Muchnoi,[10,c] H. Muramatsu,[59] S. Nakhoul,[11,f] Y. Nefedov,[29] F. Nerling,[11,f] I. B. Nikolaev,[10,c] Z. Ning,[1,49] S. Nisar,[8,i] S. L. Olsen,[54] Q. Ouyang,[1,49,54] S. Pacetti,[23b,23c] X. Pan,[9,h] Y. Pan,[58] A. Pathak,[1] P. Patteri,[23a] M. Pelizaeus,[4] H. P. Peng,[63,49] K. Peters,[11,f] J. Pettersson,[67] J. L. Ping,[34] R. G. Ping,[1,54] R. Poling,[59] V. Prasad,[63,49] H. Qi,[63,49] H. R. Qi,[52] K. H. Qi,[25] M. Qi,[35] T. Y. Qi,[9] T. Y. Qi,[2] S. Qian,[1,49] W. B. Qian,[54] Z. Qian,[50] C. F. Qiao,[54] L. Q. Qin,[12] X. P. Qin,[9] X. S. Qin,[41] Z. H. Qin,[1,49] J. F. Qiu,[1] S. Q. Qu,[36] K. H. Rashid,[65] K. Ravindran,[21] C. F. Redmer,[28] A. Rivetti,[66c] V. Rodin,[55] M. Rolo,[66c] G. Rong,[1,54] Ch. Rosner,[15] M. Rump,[60] H. S. Sang,[63] A. Sarantsev,[29,d] Y. Schelhaas,[28] C. Schnier,[4] K. Schoenning,[67] M. Scodeggio,[24a,24b] D. C. Shan,[46] W. Shan,[19] X. Y. Shan,[63,49] J. F. Shangguan,[46] M. Shao,[63,49] C. P. Shen,[9] P. X. Shen,[36] X. Y. Shen,[1,54] H. C. Shi,[63,49] R. S. Shi,[1,54] X. Shi,[1,49] X. D. Shi,[63,49] J. J. Song,[41] W. M. Song,[27,1] Y. X. Song,[38,k] S. Sosio,[66a,66c] S. Spataro,[66a,66c] K. X. Su,[68] P. P. Su,[46] F. F. Sui,[41] G. X. Sun,[1] H. K. Sun,[1] J. F. Sun,[16] L. Sun,[68] S. S. Sun,[1,54] T. Sun,[1,54] W. Y. Sun,[27] W. Y. Sun,[34] X. Sun,[20,l] Y. J. Sun,[63,49] Y. K. Sun,[63,49] Y. Z. Sun,[1] Z. T. Sun,[1] Y. H. Tan,[68] Y. X. Tan,[63,49] C. J. Tang,[45] G. Y. Tang,[1] J. Tang,[50] J. X. Teng,[63,49] V. Thoren,[67] W. H. Tian,[43] I. Uman,[53b] B. Wang,[1] C. W. Wang,[35] D. Y. Wang,[38,k] H. J. Wang,[31] H. P. Wang,[1,54] K. Wang,[1,49] L. L. Wang,[1] M. Wang,[41] M. Z. Wang,[38,k] Meng Wang,[1,54] W. Wang,[50] W. H. Wang,[68] W. P. Wang,[63,49] X. Wang,[38,k] X. F. Wang,[31] X. L. Wang,[9,h] Y. Wang,[50] Y. Wang,[63,49] Y. D. Wang,[37] Y. F. Wang,[1,49,54] Y. Q. Wang,[1] Y. Y. Wang,[31] Z. Wang,[1,49] Z. Y. Wang,[1] Ziyi Wang,[54] Zongyuan Wang,[1,54] D. H. Wei,[12] P. Weidenkaff,[28] F. Weidner,[60] S. P. Wen,[1] D. J. White,[58] U. Wiedner,[4] G. Wilkinson,[61] M. Wolke,[67] L. Wollenberg,[4] J. F. Wu,[1,54] L. H. Wu,[1] L. J. Wu,[1,54] X. Wu,[9,h] Z. Wu,[1,49] L. Xia,[63,49] H. Xiao,[9,h] S. Y. Xiao,[1] Z. J. Xiao,[34] X. H. Xie,[38,k] Y. G. Xie,[1,49] Y. H. Xie,[6] T. Y. Xing,[1,54] G. F. Xu,[1] Q. J. Xu,[14] W. Xu,[1,54] X. P. Xu,[46] Y. C. Xu,[54] F. Yan,[9,h] L. Yan,[9,h] W. B. Yan,[63,49] W. C. Yan,[71] Xu Yan,[46] H. J. Yang,[42,g] H. X. Yang,[1] L. Yang,[43] S. L. Yang,[54] Y. X. Yang,[12] Yifan Yang,[1,54] Zhi Yang,[25] M. Ye,[1,49] M. H. Ye,[7] J. H. Yin,[1] Z. Y. You,[50] B. X. Yu,[1,49,54] C. X. Yu,[36] G. Yu,[1,54] J. S. Yu,[20,l] T. Yu,[64] C. Z. Yuan,[1,54] L. Yuan,[2] X. Q. Yuan,[38,k] Y. Yuan,[1] Z. Y. Yuan,[50] C. X. Yue,[32] A. Yuncu,[53a,a]

A. A. Zafar,[65] Y. Zeng,[20,l] B. X. Zhang,[1] Guangyi Zhang,[16] H. Zhang,[63] H. H. Zhang,[50] H. H. Zhang,[27] H. Y. Zhang,[1,49]
J. J. Zhang,[43] J. L. Zhang,[69] J. Q. Zhang,[34] J. W. Zhang,[1,49,54] J. Y. Zhang,[1] J. Z. Zhang,[1,54] Jianyu Zhang,[1,54]
Jiawei Zhang,[1,54] L. Q. Zhang,[50] Lei Zhang,[35] S. Zhang,[50] S. F. Zhang,[35] Shulei Zhang,[20,l] X. D. Zhang,[37] X. Y. Zhang,[41]
Y. Zhang,[61] Y. H. Zhang,[1,49] Y. T. Zhang,[63,49] Yan Zhang,[63,49] Yao Zhang,[1] Yi Zhang,[9,h] Z. H. Zhang,[6] Z. Y. Zhang,[68]
G. Zhao,[1] J. Zhao,[32] J. Y. Zhao,[1,54] J. Z. Zhao,[1,49] Lei Zhao,[63,49] Ling Zhao,[1] M. G. Zhao,[36] Q. Zhao,[1] S. J. Zhao,[71]
Y. B. Zhao,[1,49] Y. X. Zhao,[25] Z. G. Zhao,[63,49] A. Zhemchugov,[29,b] B. Zheng,[64] J. P. Zheng,[1,49] Y. Zheng,[38,k] Y. H. Zheng,[54]
B. Zhong,[34] C. Zhong,[64] L. P. Zhou,[1,54] Q. Zhou,[1,54] X. Zhou,[68] X. K. Zhou,[54] X. R. Zhou,[63,49] A. N. Zhu,[1,54]
J. Zhu,[36] K. Zhu,[1] K. J. Zhu,[1,49,54] S. H. Zhu,[62] T. J. Zhu,[69] W. J. Zhu,[36] W. J. Zhu,[9,h] Y. C. Zhu,[63,49]
Z. A. Zhu,[1,54] B. S. Zou,[1] and J. H. Zou[1]

(BESIII Collaboration)

[1]*Institute of High Energy Physics, Beijing 100049, People's Republic of China*
[2]*Beihang University, Beijing 100191, People's Republic of China*
[3]*Beijing Institute of Petrochemical Technology, Beijing 102617, People's Republic of China*
[4]*Bochum Ruhr-University, D-44780 Bochum, Germany*
[5]*Carnegie Mellon University, Pittsburgh, Pennsylvania 15213, USA*
[6]*Central China Normal University, Wuhan 430079, People's Republic of China*
[7]*China Center of Advanced Science and Technology, Beijing 100190, People's Republic of China*
[8]*COMSATS University Islamabad, Lahore Campus, Defence Road,*
Off Raiwind Road, 54000 Lahore, Pakistan
[9]*Fudan University, Shanghai 200443, People's Republic of China*
[10]*G.I. Budker Institute of Nuclear Physics SB RAS (BINP), Novosibirsk 630090, Russia*
[11]*GSI Helmholtzcentre for Heavy Ion Research GmbH, D-64291 Darmstadt, Germany*
[12]*Guangxi Normal University, Guilin 541004, People's Republic of China*
[13]*Guangxi University, Nanning 530004, People's Republic of China*
[14]*Hangzhou Normal University, Hangzhou 310036, People's Republic of China*
[15]*Helmholtz Institute Mainz, Johann-Joachim-Becher-Weg 45, D-55099 Mainz, Germany*
[16]*Henan Normal University, Xinxiang 453007, People's Republic of China*
[17]*Henan University of Science and Technology, Luoyang 471003, People's Republic of China*
[18]*Huangshan College, Huangshan 245000, People's Republic of China*
[19]*Hunan Normal University, Changsha 410081, People's Republic of China*
[20]*Hunan University, Changsha 410082, People's Republic of China*
[21]*Indian Institute of Technology Madras, Chennai 600036, India*
[22]*Indiana University, Bloomington, Indiana 47405, USA*
[23a]*INFN Laboratori Nazionali di Frascati, I-00044, Frascati, Italy*
[23b]*INFN Sezione di Perugia, I-06100, Perugia, Italy*
[23c]*University of Perugia, I-06100, Perugia, Italy*
[24a]*INFN Sezione di Ferrara, I-44122, Ferrara, Italy*
[24b]*University of Ferrara, I-44122, Ferrara, Italy*
[25]*Institute of Modern Physics, Lanzhou 730000, People's Republic of China*
[26]*Institute of Physics and Technology, Peace Ave. 54B, Ulaanbaatar 13330, Mongolia*
[27]*Jilin University, Changchun 130012, People's Republic of China*
[28]*Johannes Gutenberg University of Mainz, Johann-Joachim-Becher-Weg 45, D-55099 Mainz, Germany*
[29]*Joint Institute for Nuclear Research, 141980 Dubna, Moscow region, Russia*
[30]*Justus-Liebig-Universitaet Giessen, II. Physikalisches Institut, Heinrich-Buff-Ring 16,*
D-35392 Giessen, Germany
[31]*Lanzhou University, Lanzhou 730000, People's Republic of China*
[32]*Liaoning Normal University, Dalian 116029, People's Republic of China*
[33]*Liaoning University, Shenyang 110036, People's Republic of China*
[34]*Nanjing Normal University, Nanjing 210023, People's Republic of China*
[35]*Nanjing University, Nanjing 210093, People's Republic of China*
[36]*Nankai University, Tianjin 300071, People's Republic of China*
[37]*North China Electric Power University, Beijing 102206, People's Republic of China*
[38]*Peking University, Beijing 100871, People's Republic of China*
[39]*Qufu Normal University, Qufu 273165, People's Republic of China*
[40]*Shandong Normal University, Jinan 250014, People's Republic of China*

[41]*Shandong University, Jinan 250100, People's Republic of China*
[42]*Shanghai Jiao Tong University, Shanghai 200240, People's Republic of China*
[43]*Shanxi Normal University, Linfen 041004, People's Republic of China*
[44]*Shanxi University, Taiyuan 030006, People's Republic of China*
[45]*Sichuan University, Chengdu 610064, People's Republic of China*
[46]*Soochow University, Suzhou 215006, People's Republic of China*
[47]*South China Normal University, Guangzhou 510006, People's Republic of China*
[48]*Southeast University, Nanjing 211100, People's Republic of China*
[49]*State Key Laboratory of Particle Detection and Electronics,*
Beijing 100049, Hefei 230026, People's Republic of China
[50]*Sun Yat-Sen University, Guangzhou 510275, People's Republic of China*
[51]*Suranaree University of Technology, University Avenue 111,*
Nakhon Ratchasima 30000, Thailand
[52]*Tsinghua University, Beijing 100084, People's Republic of China*
[53a]*Turkish Accelerator Center Particle Factory Group, Istanbul Bilgi University,*
34060 Eyup, Istanbul, Turkey
[53b]*Near East University, Nicosia, North Cyprus, Mersin 10, Turkey*
[54]*University of Chinese Academy of Sciences, Beijing 100049, People's Republic of China*
[55]*University of Groningen, NL-9747 AA Groningen, Netherlands*
[56]*University of Hawaii, Honolulu, Hawaii 96822, USA*
[57]*University of Jinan, Jinan 250022, People's Republic of China*
[58]*University of Manchester, Oxford Road, Manchester M13 9PL, United Kingdom*
[59]*University of Minnesota, Minneapolis, Minnesota 55455, USA*
[60]*University of Muenster, Wilhelm-Klemm-Str. 9, 48149 Muenster, Germany*
[61]*University of Oxford, Keble Rd, Oxford OX13RH, United Kingdom*
[62]*University of Science and Technology Liaoning, Anshan 114051, People's Republic of China*
[63]*University of Science and Technology of China, Hefei 230026, People's Republic of China*
[64]*University of South China, Hengyang 421001, People's Republic of China*
[65]*University of the Punjab, Lahore-54590, Pakistan*
[66a]*University of Turin and INFN, University of Turin, I-10125, Turin, Italy*
[66b]*University of Eastern Piedmont, I-15121, Alessandria, Italy*
[66c]*INFN, I-10125, Turin, Italy*
[67]*Uppsala University, Box 516, SE-75120 Uppsala, Sweden*
[68]*Wuhan University, Wuhan 430072, People's Republic of China*
[69]*Xinyang Normal University, Xinyang 464000, People's Republic of China*
[70]*Zhejiang University, Hangzhou 310027, People's Republic of China*
[71]*Zhengzhou University, Zhengzhou 450001, People's Republic of China*

[a]Also at Bogazici University, 34342 Istanbul, Turkey.
[b]Also at the Moscow Institute of Physics and Technology, Moscow 141700, Russia.
[c]Also at the Novosibirsk State University, Novosibirsk, 630090, Russia.
[d]Also at the NRC "Kurchatov Institute," PNPI, 188300, Gatchina, Russia.
[e]Also at Istanbul Arel University, 34295 Istanbul, Turkey.
[f]Also at Goethe University Frankfurt, 60323 Frankfurt am Main, Germany.
[g]Also at Key Laboratory for Particle Physics, Astrophysics and Cosmology, Ministry of Education; Shanghai Key Laboratory for Particle Physics and Cosmology; Institute of Nuclear and Particle Physics, Shanghai 200240, People's Republic of China.
[h]Also at Key Laboratory of Nuclear Physics and Ion-beam Application (MOE) and Institute of Modern Physics, Fudan University, Shanghai 200443, People's Republic of China.
[i]Also at Harvard University, Department of Physics, Cambridge, Massachusetts 02138, USA.
[j]Currently at Institute of Physics and Technology, Peace Ave.54B, Ulaanbaatar 13330, Mongolia.
[k]Also at State Key Laboratory of Nuclear Physics and Technology, Peking University, Beijing 100871, People's Republic of China.
[l]School of Physics and Electronics, Hunan University, Changsha 410082, China.
[m]Also at Guangdong Provincial Key Laboratory of Nuclear Science, Institute of Quantum Matter, South China Normal University, Guangzhou 510006, China.

A search for the charged lepton flavor violating decay $J/\psi \to e^\pm \tau^\mp$ with $\tau^\mp \to \pi^\mp \pi^0 \nu_\tau$ is performed with about 10×10^9 J/ψ events collected with the BESIII detector at the BEPCII. No significant signal is observed, and an upper limit is set on the branching fraction $\mathcal{B}(J/\psi \to e^\pm \tau^\mp) < 7.5 \times 10^{-8}$ at the 90% confidence level. This improves the previously published limit by two orders of magnitude.

I. INTRODUCTION

In the Standard Model (SM) of particle physics, the charged lepton flavor violating (CLFV) process is forbidden [1,2], therefore any significant sign of a signal could indicate physics beyond the SM. In recent years, there have been active phenomenological exploration of the sources of lepton flavor symmetry breaking. Many physics models beyond the SM could allow CLFV processes to take place, such as supersymmetry [3–6], the two Higgs doublet model [7,8], and models including a fourth generation of quarks and leptons [9]. The searches have been carried out in a variety of experimental endeavors. For example, the MEG collaboration searched for the decay $\mu^+ \to \gamma e^+$ and set the best upper limit (UL) of $\mathcal{B}(\mu^+ \to \gamma e^+) < 4.2 \times 10^{-13}$ [10] up to now, while the *BABAR* collaboration found a limit of $\mathcal{B}(\tau^+ \to \gamma e^+) < 3.3 \times 10^{-8}$ [11]. Meanwhile, many experiments searched for CLFV processes in the decays of pseudoscalar mesons, vector mesons, gauge bosons, and the Higgs boson, e.g., pions [12], kaons [13], B mesons [14,15], bottomonium states [16,17], Z^0 [18,19], and Higgs [20,21].

There are various theoretical predictions on CLFV in the charmonium states using model-independent methods [22,23], unparticle physics [24], and the minimal supersymmetric model with gauged baryon number and lepton number [25], etc. Some of these predictions constrain $\mathcal{B}(J/\psi \to e^\pm \mu^\mp)$ to the order of 10^{-13}, while $\mathcal{B}(J/\psi \to e^\pm \tau^\mp)$ and $\mathcal{B}(J/\psi \to \mu^\pm \tau^\mp)$ to 10^{-9}. With 58×10^6 J/ψ events, the BES collaboration obtained experimental ULs of various decays of charmonium states, namely $\mathcal{B}(J/\psi \to e^\pm \mu^\mp) < 1.1 \times 10^{-6}$ [26], $\mathcal{B}(J/\psi \to e^\pm \tau^\mp) < 8.3 \times 10^{-6}$, and $\mathcal{B}(J/\psi \to \mu^\pm \tau^\mp) < 2.0 \times 10^{-6}$ [27]. More recently and based on 225×10^6 J/ψ events collected with BESIII, an UL of $\mathcal{B}(J/\psi \to e^\pm \mu^\mp) < 1.6 \times 10^{-7}$ was obtained [28].

In this paper, the CLFV process of $J/\psi \to e^\pm \tau^\mp$ with $\tau^\mp \to \pi^\mp \pi^0 \nu_\tau$ is probed based on 10×10^9 J/ψ events collected with the BESIII detector. A semiblind analysis is performed to avoid a possible bias. About 10% of the full data sample are randomly selected. Besides the selected data, several simulation samples and independent continuum data samples are used to optimize the event selection criteria, study the background, and estimate the systematic uncertainties. The final results are obtained with the full data sample by repeating the validated analysis strategy. In the rest of this paper, the charge conjugated channel is implied unless otherwise specified.

II. BESIII DETECTOR

The BESIII detector is a magnetic spectrometer [29] located at the Beijing Electron Positron Collider (BEPCII) [30,31]. The cylindrical core of the BESIII detector consists of a helium-based multilayer drift chamber (MDC), a plastic scintillator time-of-flight system (TOF), and a CsI (Tl) electromagnetic calorimeter (EMC), which are all enclosed in a superconducting solenoidal magnet providing a 1.0 T (0.9 T in 2012) magnetic field. The solenoid is supported by an octagonal flux-return yoke with resistive plate counter muon identifier modules interleaved with steel. The acceptance of charged particles and photons is 93% over 4π solid angle. The charged-particle momentum resolution at 1 GeV/c is 0.5%, and the dE/dx resolution is 6% for the electrons from Bhabha scattering. The EMC measures photon energies with a resolution of 2.5%(5%) at 1 GeV in the barrel (end cap) region. The time resolution of the TOF barrel part is 68 ps, while that of the end cap part is 110 ps. The end cap TOF system is upgraded in 2015 with a multigap resistive plate chamber technology, providing a time resolution of 60 ps [32].

III. DATA SAMPLES AND MONTE CARLO SIMULATION

The analysis is based on J/ψ events collected in the years of 2009, 2012, 2018, and 2019 at BESIII. The total number of J/ψ events collected in these years is determined using inclusive J/ψ decays with the method described in Ref. [33]. For the selected inclusive J/ψ events, the background due to QED processes, beam-gas interactions and cosmic rays is estimated using the continuum data samples at $\sqrt{s} = 3.08$ GeV. The detection efficiency for the inclusive J/ψ decays is obtained using the experimental data sample of $\psi(3686) \to \pi^+ \pi^- J/\psi$. The efficiency difference between the J/ψ produced at rest and the J/ψ from the decay $\psi(3686) \to \pi^+ \pi^- J/\psi$ is estimated by comparing the corresponding efficiencies in a Monte Carlo (MC) simulation. The uncertainties related to the signal MC model, track reconstruction efficiency, fit to the J/ψ mass peak, background estimation, noise mixing, and reconstruction efficiency for the pions recoiling against the J/ψ are studied. Finally, the number of J/ψ events collected at BESIII is determined to be

$N_{J/\psi} = (10087 \pm 44) \times 10^6$. Among them, in 2009 and 2012, the total J/ψ number is $(1310.6 \pm 7.0) \times 10^6$ [33] and this data sample is denoted as "data sample I." Likewise, the data sample collected in 2018 and 2019 is denoted as "data sample II."

MC simulated samples produced with the GEANT4-based [34] package, which includes the geometric description of the BESIII detector and the detector response, are used to determine the detection efficiency and to estimate the backgrounds. The simulation takes the beam-energy spread and initial-state radiation in the e^+e^- annihilations into account, modeled with the generator KKMC [35]. The inclusive MC fsample consists of the production of the J/ψ resonance and the continuum processes incorporated in KKMC [35]. The inclusive MC sample contains 1.225×10^9 J/ψ events for data sample I and 8.700×10^9 J/ψ events for data sample II. The known decay modes are modeled with EvtGen [36] using branching fractions (BFs) taken from the Particle Data Group (PDG) [37], and the remaining unknown decays from the J/ψ with LUNDCHARM [38]. The final-state radiations (FSR) from charged final-state particles are incorporated with the PHOTOS package [39]. The VLL model, which describes the decay of a vector meson to two charged leptons [36], is used to generate the process $J/\psi \to e^-\tau^+$. The TAUHADNU generator, which describes the τ semileptonic decay with several pions [36], is used to generate the process $\tau^+ \to \pi^+\pi^0\nu$. This generator is based on conserved vector currents and a chiral Lagrangian model [40] with parameters taken from the paper of the CLEO collaboration [41]. The MC-generated samples simulating signal events, in the following abbreviated as signal MC samples, are generated individually for each data sample and denoted as "signal sample I" and "signal sample II". To study background contributions, many potential backgrounds of J/ψ decays are generated exclusively with a much larger statistics than each data sample, such as $J/\psi \to \pi^+\pi^-\pi^0$ with Dalitz amplitudes, $J/\psi \to \rho\pi$ with helicity amplitudes, as well as $J/\psi \to \omega f_2(1270)$ and $\bar{p}n\pi^+$ with phase space distributions.

IV. EVENT SELECTION

Two charged particles with zero net charge are required to satisfy the polar-angle condition $|\cos\theta| < 0.8$ with respect to the beam axis. Their closest approaches to the interaction point are required to be within 10 cm in the beam direction and within 1 cm in the plane perpendicular to the beam. The particle identification (PID) is performed by combining the energy-loss measurement, dE/dx, obtained from the MDC and the time-of-flight information from the TOF. PID confidence levels (C.L.) are calculated for the electron (CL_e), pion (CL_π), proton (CL_p), and kaon (CL_K) hypotheses. The electron (pion) candidate requires the electron (pion) hypothesis to have the highest PID

confidence levels among the four hypotheses. For electron candidates, the $CL_e/(CL_e + CL_\pi)$ ratio is required to be larger than 0.95 and the E/p is larger than 0.8 to further improve the electron identification. Here, the variables E and p refer to the energy deposition of the charged track in the EMC and its momentum measured with the MDC, respectively.

Electromagnetic showers in the EMC are identified as photon candidates only if the following criteria are satisfied. The energy deposition is required to be larger than 25 MeV in the barrel ($|\cos\theta| < 0.8$) region and 50 MeV in the end cap ($0.86 < |\cos\theta| < 0.92$) regions. To eliminate showers produced by charged particles, the photon candidates are required to be separated from the extrapolated positions of any charged track by more than $10°$. To suppress electronic noise and unrelated energy depositions, the EMC time deviation from the event start time is required to be within 700 ns. At least two photons satisfying these selection criteria are required in the final state. The π^0 candidate is reconstructed from photon pairs whose invariant mass $M(\gamma\gamma)$ is required to satisfy 115 MeV/$c^2 < M(\gamma\gamma) < 150$ MeV/c^2. To improve the momentum resolution, a kinematic fit is applied by constraining the two-photon invariant mass to the nominal π^0 mass, and the refined four momenta of the photons are used for further analysis.

The final-state electron from the process $J/\psi \to e^-\tau^+$ is monochromatic, therefore the momentum of the electron P_e and the recoiling mass against the electron M_{e_recoil} are required to be within 1.009 GeV/$c < P_e < 1.068$ GeV/c and 1.742 GeV/$c^2 < M_{e\_recoil} < 1.811$ GeV/c^2, respectively. The momentum and recoil-mass resolutions are found, using MC simulations, to be 0.010 and 0.011 GeV/c^2, respectively. Figure 1 compares the momentum and recoil-mass distributions of the complete data sample with the corresponding signal MC simulation and J/ψ inclusive MC samples. The possible background from continuum process would be discussed in the next section.

The missing energy E_{miss} is calculated by $E_{miss} = E_{CMS} - E_e - E_\pi - E_{\pi^0}$, where E_{CMS} is the center-of-mass energy of the initial e^+e^- system, while E_e, E_π, and E_{π^0} are the energies of the electron, charged pion, and neutral pion in the rest frame of the e^+e^- system. The E_{miss} is required to be larger than 0.43 GeV to suppress the background events whose final states are all detected. The variable U_{miss}, calculated by $U_{miss} = E_{miss} - c|\vec{P}_{miss}|$, is used to define the signal region to have a better resolution than the missing mass. The variable $\vec{P}_{miss} = \vec{P}_{J/\psi} - \vec{P}_e - \vec{P}_\pi - \vec{P}_{\pi^0}$ is the missing momentum, where $\vec{P}$ are the corresponding momenta in the rest frame of the e^+e^- system of the particles indicated by the subscript. As the signal events peak near zero with one undetected neutrino, the signal region is defined to be -0.081 GeV $< U_{miss} < 0.112$ GeV,
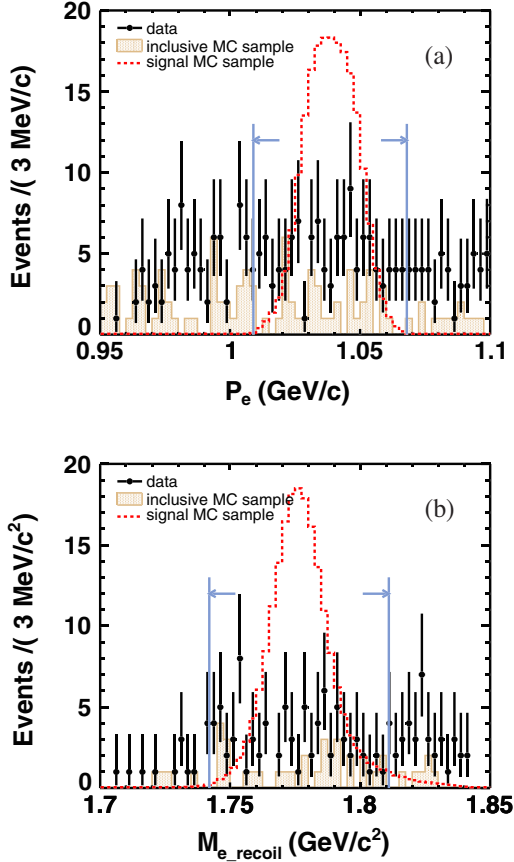
FIG. 1. (a) The electron-momentum P_e and (b) recoil-mass M_{e_recoil} distributions. The dots with error bars are data, while the shaded histograms are obtained from a J/ψ inclusive MC sample normalized to data. The dashed lines show the arbitrarily scaled signal shape extracted from the MC signal samples. The areas between the arrows indicate the selection region.

which corresponds to three standard deviations of the expected width determined from the signal MC sample. The number of signal candidates for each data sample, $N_{\rm obs}$, is obtained by counting the number of entries that fall within the signal region. After applying the above selection criteria, the detection efficiency of the signal sample I (II) is determined to be $(20.24 \pm 0.05)\%$ $((19.37 \pm 0.02)\%)$.

V. BACKGROUND STUDY

The dominant background contaminations stem from the continuum process (e.g. radiative Bhabha) and from hadronic J/ψ decays such as $J/\psi \to \pi^+\pi^-\pi^0$.

The continuum background is studied with a 150 pb^{-1} data sample collected at $\sqrt{s} = 3.08$ GeV and a 2.93 fb^{-1} data sample taken at $\sqrt{s} = 3.773$ GeV. The survived events are dominated by radiative Bhabha process, therefore the normalized background events from the continuum processes are estimated with the assumption of a $1/s$ dependence of the cross section. Radiative Bhabha MC samples at different energy points are used to evaluate the

uncertainty of this assumption to be about 24%. Single electron MC samples are used to study the electron momentum resolution differences at different energy points. The resolution differences are applied to radiative Bhabha MC samples, and the result shows this influence could be negligible in this study. The continuum background events are estimated to be 5.8 ± 1.8 (37.9 ± 11.5) for data sample I (II) with the uncertainties of statistics and the assumption of $1/s$ dependence taken into consideration.

The J/ψ decay background is studied with the inclusive MC samples, and only a few events survive. Main background processes from $J/\psi \to \pi^+\pi^-\pi^0$, $J/\psi \to \rho\pi$, $J/\psi \to \omega f_2(1270)$, and $J/\psi \to \bar{p}n\pi^+$ are studied with exclusive MC samples. The uncertainty in the J/ψ decay modeling is determined to be about 16% from the inclusive MC samples with and without LUNDCHARM model. The normalized background events from the J/ψ decays are estimated to be 1.1 ± 0.8 (25.7 ± 6.4) for data sample I (II) with statistical and J/ψ decay modeling uncertainties taken into consideration. The possible cross feed from the CLFV process $J/\psi \to e^\pm\tau^\mp$ whereby the τ decays to other modes has been studied using a τ inclusive MC sample modeled by EvtGen [36] and found to be negligible (0.3%). The background events from J/ψ decay processes are normalized according to the BFs from the PDG [37], the number of J/ψ events, and the detection efficiencies determined from the exclusive MC samples.

The normalized background events from continuum processes and J/ψ decay processes discussed above are utilized to estimate the number of background events left in the signal region. In total, 6.9 ± 1.9 (63.6 ± 13.2) background events are expected for the data sample I (II). Some
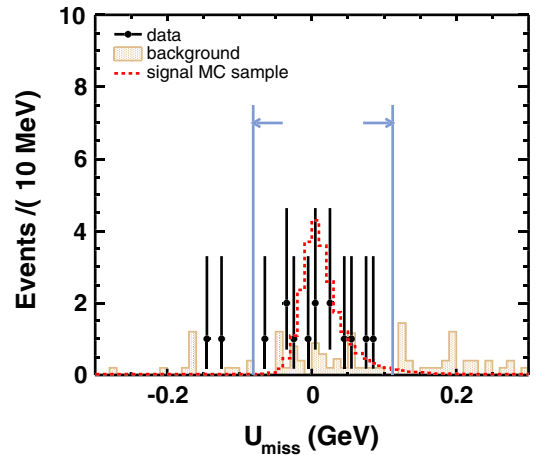

FIG. 2. The $U_{\rm miss}$ distribution of data sample I and corresponding background. The dots with error bars are data, while the shaded histogram is from the normalized continuum sample as well as the J/ψ inclusive MC samples. The dashed line shows the arbitrarily scaled signal MC shape extracted from the signal sample I. The areas between the arrows represent the signal region.
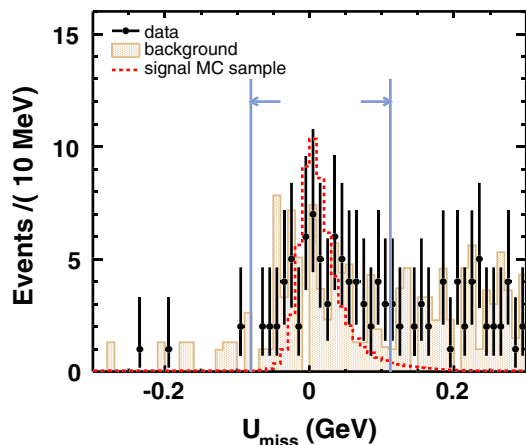
FIG. 3.   Same as Fig. 2 except for data sample II and signal sample II.

background events with additional soft tracks contribute near the $U_{\text{miss}} = 0$ region. The signal region is opened after completing the optimization of the analysis algorithms and the background study. Figures 2 and 3 depict U_{miss} for the data samples I and II, respectively.

VI. SYSTEMATIC UNCERTAINTIES

Systematic uncertainties mainly come from uncertainties in the total number of J/ψ decays, the quoted intermediate BF, the background estimation, and in efficiencies associated with signal modeling, PID and tracking of charged particles, the photon detection, the π^0 reconstruction, and kinematic variable requirements. The details of most of sources are described below, while the uncertainties from background estimation have been considered in the Sec. V.

The uncertainty in the number of J/ψ events is determined to be 0.5% for the data sample I [33], and 0.4% for the data sample II. The uncertainty in the quoted BF of $\tau^+ \to \pi^- \pi^0 \nu_\tau$ is 0.4% [37]. To estimate the uncertainty in the signal MC model, the generator producing $\tau^+ \to \pi^- \pi^0 \nu_\tau$ decays is changed to the TAUVECTORNU generator (for $\tau^+ \to \rho^+ \nu_\tau$) and the VSS generator (for $\rho^+ \to \pi^+ \pi^0$) [36]. The TAUVECTORNU generator simulates the decay of a τ lepton into a vector particle and a neutrino, while the VSS generator simulates the decay a vector meson into a pair of scalar particles. The relative change in the detection efficiency of signal sample I, 0.6%, is assigned as the uncertainty. The relative change in the efficiency for sample II is found to be negligible.

The uncertainty in the PID of pions is 1.0% per charged pion, as determined from a study of the control sample of the process $J/\psi \to \rho\pi$ [42]. The MDC tracking efficiency of charged pions is studied using the control sample of $J/\psi \to \pi^+ \pi^- p\bar{p}$ decays, and the difference between the data and MC simulation is 1.0% for each charged pion [43]. The PID and tracking efficiencies of electrons are obtained from a control sample of radiative Bhabha scattering

$e^+ e^- \to \gamma e^+ e^-$ (including $J/\psi \to \gamma e^+ e^-$) corresponding to the center-of-mass energy of the J/ψ resonance. For the electron-PID study, the same PID requirements as applied to the dataset of interest are exposed to the control samples. Similarly, for the electron-tracking study, we applied the same conditions for the polar angle and for the closest distance to the interaction point as was used for the data of interest. Differences in PID (tracking) efficiencies between the data and MC simulations are obtained for each bin of a two-dimensional distribution representing the momentum (transverse momentum) versus the polar angle of the electron tracks. These results are subsequently used to determine the overall weighted differences per track for PID (tracking). We obtained PID and tracking uncertainties for electrons of the signal sample I (II) of 0.4% (0.9%) and 0.1% (0.1%) per track, respectively.

The photon detection efficiency is studied with the control sample based on $J/\psi \to \pi^+ \pi^- \pi^0$, $\pi^0 \to \gamma\gamma$ events [42]. The difference between data and MC simulation is 0.5% (1.5%) for a photon in the EMC barrel (end cap) region. The average difference, 0.5% per photon, is taken as systematic uncertainty. The total systematic uncertainty due to uncertainties in the photon-detection efficiency is estimated to be 1.0%. The uncertainty related to the π^0 reconstruction is determined to be 1.0% for the two samples using a $J/\psi \to \pi^+ \pi^- \pi^0$ control sample as described in Ref. [44].

The systematic uncertainties related to P_e and M_{e_recoil} requirements are studied with the control sample of the process $e^+ e^- \to \gamma e^+ e^-$ (including $J/\psi \to \gamma e^+ e^-$) at the center-of-mass energy of the J/ψ resonance. The differences in efficiency between the data and MC simulation for these two kinematic variables are studied by varying the event-selection requirement ranges while taking into account the correlation between them. This uncertainty is determined to be 3.0% (3.3%) for sample

TABLE I.   Summary of the sources of systematic uncertainties and their estimated magnitudes. The correlated sources are marked with an asterisk, which are added linearly when combining the two data samples. The negligible uncertainty is marked with a dash line.

Sources	Sample I	Sample II
Number of J/ψ	0.5%	0.4%
Quoted BF*	0.4%	0.4%
MC model	0.6%	...
Pion PID*	1.0%	1.0%
Pion tracking*	1.0%	1.0%
Electron PID	0.4%	0.9%
Electron tracking*	0.1%	0.1%
Photon detection*	1.0%	1.0%
π^0 reconstruction*	1.0%	1.0%
P_e and M_{e_recoil} requirements	3.0%	3.3%
E_{miss} requirement	1.0%	0.8%
Total uncertainty	3.9%	4.1%

TABLE II. A summary of the analysis results. See the text for details.

Results	Sample I	Sample II
N_{obs}	13	69
$N_{\text{bkg}}^{\text{exp}}$	6.9	63.6
$\sigma_{\text{bkg}}^{\text{exp}}$	1.9	13.2
$\epsilon_{\text{eff}}^{\text{mc}}$	20.24%	19.37%
$\sigma_{\text{eff}}^{\text{mc}}$	0.79%	0.79%
BF (90% C.L.)		7.5×10^{-8}

I (II). The same control sample is used to study the uncertainty associated with E_{miss} requirement. The electron with the lowest momentum is assumed to be a missing track, and the data-MC differences of the resulting missing energy are derived as correction factors to be applied to the E_{miss} distribution of the signal MC sample. Then the difference in efficiency, 1.0% (0.8%), between the signal MC sample with and without the correction is taken as the systematic uncertainty for data sample I (II).

Table I summarizes all sources of systematic uncertainties discussed above. The total systematic uncertainties of each data sample are obtained by adding these uncertainties in quadrature.

VII. RESULTS

Table II summarizes the extracted parameters of each sample. The parameters $N_{\text{bkg}}^{\text{exp}}$ and $\sigma_{\text{bkg}}^{\text{exp}}$ are the expected number of background events and its uncertainty in the signal region determined from the background study; $\epsilon_{\text{eff}}^{\text{mc}}$ and $\sigma_{\text{eff}}^{\text{mc}}$ denotes the efficiency and its uncertainty determined from signal MC samples and the study of systematic uncertainties.

Since no significant signal is observed, a maximum likelihood estimator, extended from the profile-likelihood approach [45], is used to determine the UL on the BF of $J/\psi \to e^{\pm}\tau^{\mp}$. The likelihood function of each sample which depends on the parameter of interest $\mathcal{B}(J/\psi \to e^{\pm}\tau^{\mp})$ and the nuisance parameters $\boldsymbol{\theta} = (\epsilon_{\text{eff}}, N_{\text{bkg}})$ is defined as

$$\mathcal{L}(\mathcal{B}(J/\psi \to e^{\pm}\tau^{\mp}), \boldsymbol{\theta})$$
$$= P(N_{\text{obs}}, \mathcal{B}(J/\psi \to e^{\pm}\tau^{\mp}) \cdot N_{J/\psi} \cdot \mathcal{B}_{\tau^{\mp} \to \pi^{\mp}\pi^0\nu_{\tau}} \cdot \epsilon_{\text{eff}} + N_{\text{bkg}})$$
$$\cdot G(\epsilon_{\text{eff}}^{\text{mc}}, \epsilon_{\text{eff}}, \sigma_{\text{eff}}^{\text{mc}}) \cdot G(N_{\text{bkg}}^{\text{exp}}, N_{\text{bkg}}, \sigma_{\text{bkg}}^{\text{exp}}),$$

where the observed events are assumed to follow a Poisson distribution (P), while the detection efficiency ϵ_{eff} and the background number N_{bkg} follow Gaussian distributions (G); $N_{J/\psi}$ is the number of J/ψ events.

The likelihood function is treated as the probability function, and the UL on the $J/\psi \to e^{\pm}\tau^{\mp}$ at 90% C.L. is determined by integrating the likelihood distribution in
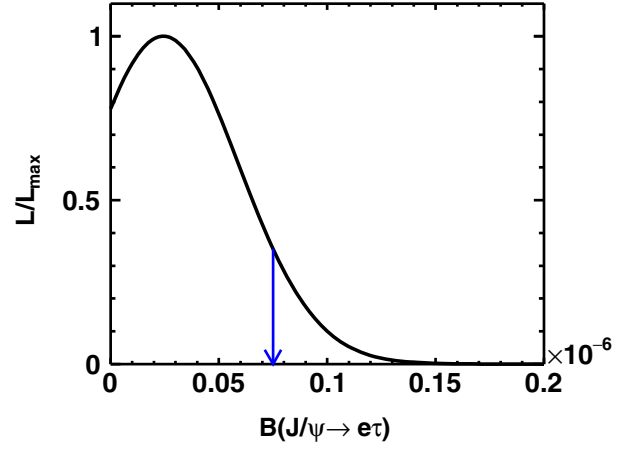

FIG. 4. The combined likelihood distribution as a function of the branching fraction of the data samples. The arrow points to the position of the UL at 90% C.L.

the physical region of $\mathcal{B} \geq 0$ based on the Bayesian method with the RooStats package [46]. The combined likelihood distribution as a function of the BF from the data samples is shown in Fig. 4. The resultant UL is $\mathcal{B}(J/\psi \to e^{\pm}\tau^{\mp}) < 7.5 \times 10^{-8}$ (90% C.L.), where the detection efficiency, statistical and systematic uncertainties as well as the background estimation are all incorporated.

VIII. SUMMARY

This paper presents a search of the CLFV process $J/\psi \to e^{\pm}\tau^{\mp}$ with $\tau^{\mp} \to \pi^{\mp}\pi^0\nu_{\tau}$ using a data sample based upon 10×10^9 J/ψ events collected with the BESIII detector. A semiblind analysis found no significant excess in the datasets with respect to the expected background. The UL is determined to be $\mathcal{B}(J/\psi \to e^{\pm}\tau^{\mp}) < 7.5 \times 10^{-8}$ (90% C.L.), where uncertainties are taken into account. This improves the previous published limits [27] by more than two orders of magnitude and can be used to constrain new physics parameter spaces.

ACKNOWLEDGMENTS

[1] W. J. Marciano and A. Sanda, Phys. Lett. **67B,** 303 (1977).

[2] W. J. Marciano, T. Mori, and J. M. Roney, Annu. Rev. Nucl. Part. Sci. **58,** 315 (2008).

[3] F. Borzumati and A. Masiero, Phys. Rev. Lett. **57,** 961 (1986).

[4] A. Arbey, M. Battaglia, A. Djouadi, F. Mahmoudi, and J. Quevilon, Phys. Lett. B **708,** 162 (2012).

[5] P. Paradisi, J. High Energy Phys. 10 (2005) 006.

[6] L. Calibbi, P. Paradisi, and R. Ziegler, Eur. Phys. J. C **74,** 3211 (2014).

[7] G. C. Branco, P. M. Ferreira, L. Lavoura, M, N. Rebelo, M. Sher, and J. P. Silva, Phys. Rep. **516,** 1 (2012).

[8] A. Crivellin, C. Greub, and A. Kokulu, Phys. Rev. D **87,** 094031 (2013).

[9] A. J. Buras, B. Duling, T. Feldmann, T. Heidsieck, and C. Promberger, J. High Energy Phys. 09 (2010) 104.

[10] A. M. Baldini et al. (MEG Collaboration), Eur. Phys. J. C **76,** 434 (2016).

[11] B. Aubert et al. (*BABAR* Collaboration), Phys. Rev. Lett. **104,** 021802 (2010).

[12] D. Ambrose et al. (BNL Collaboration), Phys. Rev. Lett. **81,** 5734 (1998).

[13] E. Abouzaid et al. (KTeV Collaboration), Phys. Rev. Lett. **100,** 131803 (2008).

[14] R. Aaij et al. (LHCb Collaboration), J. High Energy Phys. 03 (2018) 078.

[15] B. Aubert et al. (*BABAR* Collaboration), Phys. Rev. D **77,** 091104 (2008).

[16] W. Love et al. (CLEO Collaboration), Phys. Rev. Lett. **101,** 201601 (2008).

[17] J. Lees et al. (*BABAR* Collaboration), Phys. Rev. Lett. **104,** 151802 (2010).

[18] G. Aad et al. (ATLAS Collaboration), Phys. Rev. D **90,** 072010 (2014).

[19] M. Aaboud et al. (ATLAS Collaboration), Phys. Rev. D **98,** 092010 (2018).

[20] V. Khachatryan et al. (CMS Collaboration), Phys. Lett. B **763,** 472 (2016).

[21] A. M. Sirunyan et al. (CMS Collaboration), J. High Energy Phys. 06 (2018) 001.

[22] S. Nussinov, R. D. Peccei, and X. M. Zhang, Phys. Rev. D **63,** 016003 (2000).

[23] T. Gutsche, J. C. Helo, S. Kovalenko, and V. E. Lyubovitskij, Phys. Rev. D **83,** 115015 (2011).

[24] K. S. Sun, T. F. Feng, L. N. Kou, F. Sun, T. J. Gao, and H. B. Zhang, Mod. Phys. Lett. A **27,** 1250172 (2012).

[25] X. X. Dong, S. M. Zhao, J. J. Feng, G. Z. Ning, J. B. Chen, H. B. Zhang, and T. F. Feng, Phys. Rev. D **97,** 056027 (2018).

[26] J. Z. Bai et al. (BES Collaboration), Phys. Lett. B **561,** 49 (2003).

[27] M. Ablikim et al. (BES Collaboration), Phys. Lett. B **598,** 172 (2004).

[28] M. Ablikim et al. (BESIII Collaboration), Phys. Rev. D **87,** 112007 (2013).

[29] M. Ablikim et al. (BESIII Collaboration), Nucl. Instrum. Methods Phys. Res., Sect. A **614,** 345 (2010).

[30] C. H. Yu et al., BEPCII Performance and Beam Dynamics Studies on Luminosity, in *Proceedings of IPAC2016, Busan, Korea* (JACoW, Geneva, Switzerland, 2016), https://doi.org/10.18429/JACoW-IPAC2016-TUYA01.

[31] M. Ablikim et al. (BESIII Collaboration), Chin. Phys. C **44,** 040001 (2020).

[32] X. Li et al., Radiat. Detect. Technol. Methods **1,** 13 (2017); Y. X. Guo et al., Radiat. Detect. Technol. Methods **1,** 15 (2017); P. Cao et al., Nucl. Instrum. Methods Phys. Res., Sect. A **953,** 163053 (2020).

[33] M. Ablikim et al. (BESIII Collaboration), Chin. Phys. C **41,** 013001 (2017).

[34] S. Agostinelli et al. (GEANT4 Collaboration), Nucl. Instrum. Methods Phys. Res., Sect. A **506,** 250 (2003).

[35] S. Jadach, B. F. L. Ward, and Z. Was, Phys. Rev. D **63,** 113009 (2001); Comput. Phys. Commun. **130,** 260 (2000).

[36] D. J. Lange, Nucl. Instrum. Methods Phys. Res., Sect. A **462,** 152 (2001); R. G. Ping, Chin. Phys. C **32,** 599 (2008).

[37] P. A. Zyla et al. (Particle Data Group), Prog. Theor. Exp. Phys. **2020,** 083C01 (2020).

[38] J. C. Chen, G. S. Huang, X. R. Qi, D. H. Zhang, and Y. S. Zhu, Phys. Rev. D **62,** 034003 (2000); R. L. Yang, R. G. Ping, and H. Chen, Chin. Phys. Lett. **31,** 061301 (2014).

[39] E. Richter-Was, Phys. Lett. B **303,** 163 (1993).

[40] J. H. Kuhn and A. Santamaria, Z. Phys. C **48,** 445 (1990).

[41] S. Anderson *et al.* (CLEO Collaboration) Phys. Rev. D **61,** 112002 (2000).

[42] M. Ablikim *et al.* (BESIII Collaboration), Phys. Rev. D **83,** 112005 (2011).

[43] M. Ablikim *et al.* (BESIII Collaboration), Phys. Rev. Lett. **107,** 092001 (2011).

[44] M. Ablikim *et al.* (BESIII Collaboration), Phys. Rev. D **81,** 052005 (2010).

[45] W. A. Rolke, A. M. Lopez, and J. Conrad, Nucl. Instrum. Methods Phys. Res., Sect. A **551,** 493 (2005).

[46] L. Moneta *et al.*, Proc. Sci., ACAT2010 (**2010**) 057.